the substrate (i.e., dipping, cross-linking, and ready-made polymers with reactive end groups reacting with the functional groups of the substrate) [3–5].

2-Methacryloyloxyethyl phosphorylcholine (MPC) polymers have attracted considerable attention as surface modifiable polymers for several medical devices [6–16]. MPC is a monomer for preparing novel polymer biomaterials and can undergo conventional radical copolymerization with other methacrylates, such as *n*-butyl methacrylate (BMA), *n*-dodecyl methacrylate (DMA), and 3-methacryloxypropyl trimethoxysilane (MPSi), to form poly (MPC-*co*-BMA), poly(MPC-*co*-DMA), and poly(MPC-*co*-MPSi), respectively [10–16]. They have potential applications in a variety of fields such as biomedical science, surface science, and bioengineering because they possess unique properties such as excellent anti-biofouling ability and low friction ability. Thus, surface modification with the MPC polymer on medical devices is effective for obtaining biocompatibility. In fact, several medical devices have already been developed by utilizing MPC polymers and used clinically; therefore, the efficacy and safety of MPC polymers as biomaterials are well established [14–16].

In this study, we hypothesize that the structure of surface modification layers might affect the long-term stability, hydration kinetics, articular cartilage retention, etc., and particularly that the poly(MPC) (PMPC)-grafted surface might assure the long-term performance of the artificial femoral head for partial hemiarthroplasty. Therefore, we investigated the surface properties of various surface modification layers with the MPC polymer and the effects of the surface properties on the friction of the artificial femoral head against articular cartilage. The results reveal that the structure of the PMPC-grafted layer on the Co–Cr–Mo surface plays an important role in the articular cartilage retention in the long term.

2. Materials and methods

2.1. Chemicals

MPC was industrially synthesized by using the method reported by Ishihara et al. and supplied by NOF Corp. (Tokyo, Japan) [17]. MPSi was purchased from Shin-Etsu Chemical Co., Ltd. (Tokyo, Japan). Succinic acid and ethanol were purchased from Kanto Chemical Co., Inc. (Tokyo, Japan). 2-Hydroxy-1-[4-(hydroxyethoxy) phenyl]-2-methyl-propan-1-one (DAROCUR 2959; D2959), as a highly efficient radical photoinitiator for ultraviolet (UV) curing, was purchased from Ciba Specialty Chemicals Holding Inc. (Basel, Switzerland) Poly(MPC-*co*-BMA) (PMB30; MPC unit mole fraction = 0.3) [17], poly(MPC-*co*-MPSi) (PMSi90; MPC unit mole fraction = 0.9) [13], and PMPC (for lubricant additive in friction test) were synthesized in ethanol using 2,2′-azobisisobutyronitrile as an initiator by a conventional radical copolymerization method.

2.2. Co–Cr–Mo alloy substrate and pretreatments

The Co–Cr–Mo alloy was supplied by Yoneda Advanced Casting Co., Ltd (Takaoka, Japan). This alloy was manufactured according to the ASTM F75 standard specification for the Co–28Cr–6Mo alloy. The Co–Cr–Mo samples were machined and polished so that the average surface roughness was approximately 0.01 μm; this surface was comparable to those of femoral ball products.

The polished Co–Cr–Mo samples were washed with acetone, and then immersed in 35 vol% nitric acid at room temperature for 35 min. This treatment aimed at passivation by surface oxidation; this would lead to the dissolution of certain foreign substance residues and the concentration of the Cr constituent by "resurfacing" [18]. After the nitric acid treatment, the Co–Cr–Mo samples were irradiated with O_2 plasma at a 500-W high-frequency output and 150-mL/min O_2 gas flow for 5 min by using an O_2 plasma etcher (PR500; Yamato Scientific Co., Ltd., Tokyo, Japan). The O_2 plasma treatment increased the thickness of the surface oxide layer [18].

2.3. MPC polymer coating

The preparation of the MPC polymer-coated Co–Cr–Mo is schematically illustrated in Fig. 1. The physical adsorption of PMB30 was carried out by the solvent evaporation method, where the pretreated Co–Cr–Mo specimens were dipped into ethanol solution containing 0.2 mass% PMB30 ($Mw = 6.0 \times 10^5$) for 10 s for coating and then placed in an ethanol vapor atmosphere at room temperature for 1 h. The coated Co–Cr–Mo specimens were again dipped for 10 s and placed in the ethanol vapor atmosphere at room temperature for 1 h (PMB30-adsorbed Co–Cr–Mo).

The chemical immobilization of PMSi90 was also carried out by the solvent evaporation method. The pretreated Co–Cr–Mo specimens were dipped into ethanol solution containing 0.5 mass% PMSi90 ($Mw = 9.8 \times 10^4$) and 0.063 mg/mL succinic acid for 12 h for the silanization of trimethoxysilane group of PMSi90 and placed in the ethanol vapor atmosphere at room temperature for 1 h. The coated Co–Cr–Mo specimens were annealed in air at 70 °C for 3 h for dehydration (PMSi90-immobilized Co–Cr–Mo).

2.4. MPSi silanization and MPC graft polymerization

The preparation of the PMPC-grafted Co–Cr–Mo is schematically shown in Fig. 1. The pretreated Co–Cr–Mo samples were immersed in an ethanol solution containing 5 mass% MPSi, 1 mass% succinic acid, and 0.1 mass% D2959 at room temperature for 12 h for silanization of the trimethoxysilane group. In this study, D2959 was used as a photoinitiator for surface-initiated polymerization so as to be included in the MPSi layer. They were then annealed at 70 °C for 3 h in air for dehydration. MPC was dissolved in degassed pure water to obtain a concentration of 0.5 mol/L. Subsequently, the MPSi (containing D2959)-coated Co–Cr–Mo samples were immersed in MPC aqueous solutions. Photoinduced graft polymerization on the Co–Cr–Mo surface was performed using ultraviolet irradiation (UVL-400HA ultra-high pressure mercury lamp; Riko-Kagaku Sangyo Co., Ltd., Funabashi, Japan) with an intensity of 5 mW/cm^2 at 60 °C for 90 min; a filter (Model D-35; Toshiba Co., Tokyo, Japan) was used to restrict the passage of ultraviolet light to wavelengths of 350 ± 50 nm (PMPC-grafted Co–Cr–Mo) [19]. After the polymerization, the PMPC-grafted Co–Cr–Mo samples were removed from the solution, washed with pure water and ethanol, and dried at room temperature. The molecular weight of the PMPC graft chain on the PMPC-grafted Co–Cr–Mo samples could not be determined due to the difficulty in separating the PMPC graft chain from the Co–Cr–Mo substrate. Additional efforts are needed in this aspect.

2.5. Articular cartilage from porcine ankle joint

Articular cartilage specimens were harvested from the flat part of the ankle joint of the fresh frozen porcine tibia (age 6–9 months) by using a surgical saw for the friction test. The pin-type (cylinder-shaped with a height of 5 mm and diameter of 9 mm) articular cartilage specimens had approximately a 1-mm cartilage layer and the subcondral bone used for mounting. Throughout the procedure, the articular cartilage surface was hydrated regularly with Dulbecco's phosphate-buffered saline (PBS, pH 7.4, ion strength = 0.15 M; Immuno-Biological Laboratories Co., Ltd., Takasaki, Japan).

2.6. Surface analysis of surface-modified Co–Cr–Mo with various MPC polymers

The functional group vibrations of the surface-modified Co–Cr–Mo samples were examined by Fourier-transform infrared (FT-IR) spectroscopy with attenuated total reflection (ATR) equipment. The FT-IR/ATR spectra were obtained using an FT-IR analyzer (FT/IR615; JASCO Co. Ltd., Tokyo, Japan) for 32 scans over the range from 800 to 2000 cm^{-1} at a resolution of 4.0 cm^{-1}.

The surface elemental conditions of the surface-modified Co–Cr–Mo samples were analyzed by X-ray photoelectron spectroscopy (XPS). The XPS spectra were obtained using an XPS spectrophotometer (AXIS-HSi165, Kratos/Shimadzu Co., Kyoto, Japan) equipped with a 15-kV Mg-Kα radiation source at the anode. The take-off angle of the photoelectrons was maintained at 90°. Five scans were taken for each sample.

The static-water contact angles on the surface-modified Co–Cr–Mo samples were measured by the sessile drop method using an optical bench-type contact angle goniometer (Model DM300, Kyowa Interface Science Co., Ltd., Saitama, Japan). Drops of purified water (1 μL) were deposited on the surface-modified Co–Cr–Mo surfaces, and the contact angles were directly measured with a microscope after 60 s of dropping. Measurements were repeated fifteen times for each sample, and the average values were regarded as the contact angles.

The surface-modified Co–Cr–Mo samples were stained with rhodamine 6G (Wako Pure Chemical Industries, Ltd., Osaka, Japan) and observed by fluorescence microscopy (FM). According to previous literature, rhodamine 6G effectively stains the MPC polymer, which possesses great structural similarity to lipids [20]. This simple staining technique enables the evaluation of the surface-modified layer with MPC polymer by FM. An aqueous solution of 200 mass ppm rhodamine 6G was used for all the staining experiments. The samples were immersed in the rhodamine 6G solution for 30 s and then removed. Then, they were washed two times consecutively in distilled water for 30 s and then dried. A fluorescence microscope (Axioskop 2 Plus, Carl Zeiss AG, Oberkochen, Germany) was used for FM imaging and examination of all samples. Pseudo-color images were obtained using a charge coupled device (CCD) camera (VB-7010, Keyence Co., Osaka, Japan) and imaging software (VH analyzer 2.51). Lenses with ×10 magnification and appropriate exposure time (approximately 0.1 s) were employed to obtain the best image quality of the various samples.

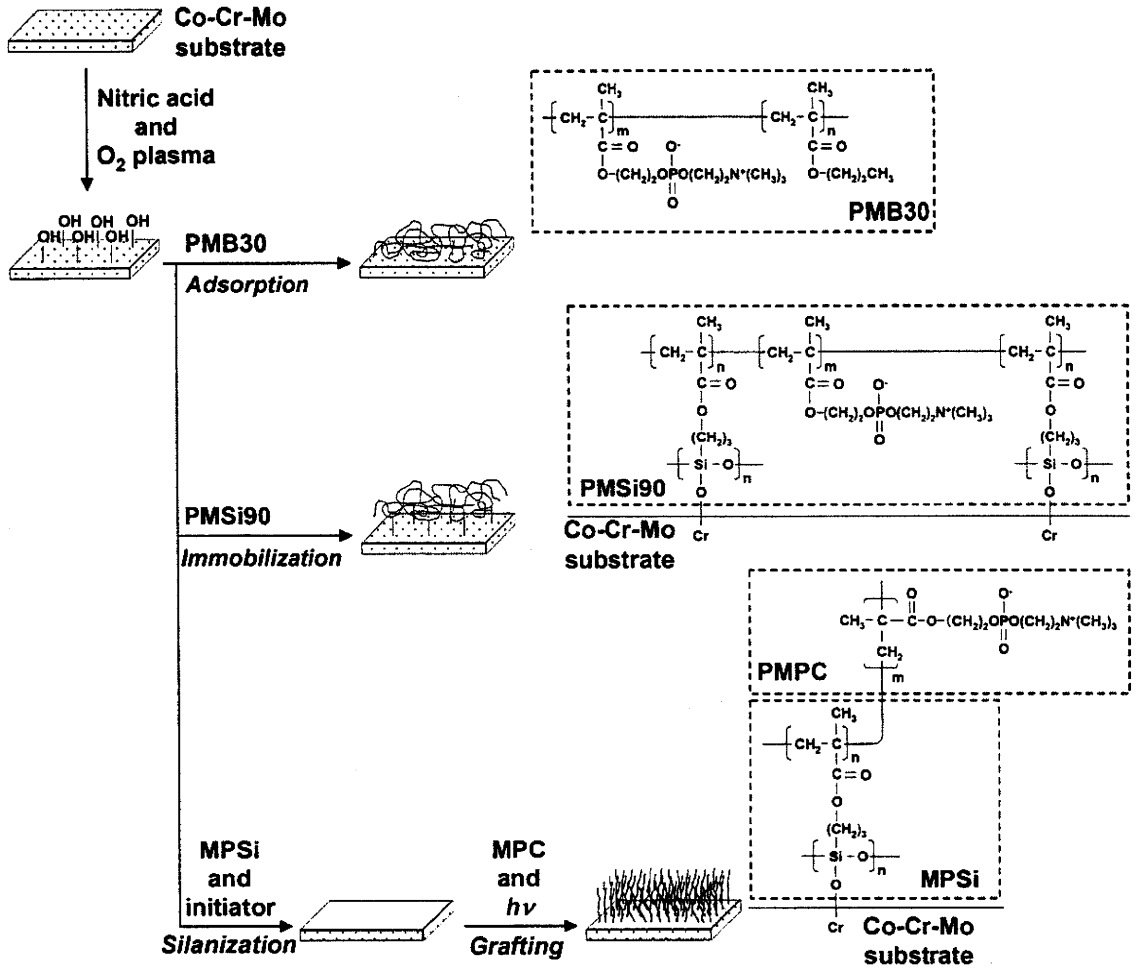

Fig. 1. Schematic illustration for the preparation of MPC polymer-coated and PMPC-grafted Co–Cr–Mo.

2.7. Cross-sectional observation by transmission electron microscopy

A cross-section of the surface-modified Co–Cr–Mo samples was observed using a transmission electron microscope (TEM) and by energy dispersive X-ray (EDX) spectroscopy. The specimens were precoated with an aluminum film; then, a thin film of the samples was prepared by the focused ion beam (FIB) technique using an FB-2000A (Hitachi High-Technologies Co., Tokyo, Japan) FIB system. The samples were thinned to electron transparency by a low gallium ion beam current. The thin film thus prepared was positioned onto a copper TEM mesh grid. TEM observations were then recorded using an HF-2000 electron microscope (Hitachi High-Technologies Co.) at an acceleration voltage of 200 kV. EDX spectra were analyzed on a cross-section of the samples using a Sigma EDX attachment (Kevex Instruments, Inc., Valencia, CA, USA) at an acceleration voltage of 200 kV.

2.8. Characterization of protein adsorption by micro bicinchoninic acid method

The amounts of protein adsorbed on the surface-modified Co–Cr–Mo samples were determined by the micro bicinchoninic acid (BCA) method. Each specimen was immersed in PBS for 1 h to equilibrate the surface modified by the MPC polymer. The specimens were immersed in bovine serum albumin (BSA, Mw = 6.7×10^4; Sigma–Aldrich Corp., MO, USA), bovine blood γ-globulins (Mw = 1.5×10^5; Sigma–Aldrich Co.), and bovine plasma fibrinogen (Mw = 3.4×10^5; Sigma–Aldrich Co.) solutions at 37 °C for 1 h. The protein solutions were prepared in BSA, γ-globulins, and fibrinogen concentrations of 4.5, 1.6, and 0.3 g/L, respectively, i.e., 10% of the concentration of human plasma levels. Then, the specimens were rinsed five times with fresh PBS and immersed in 1 mass% sodium dodecyl sulfate (SDS) aqueous solution and shaken at room temperature for 1 h to completely detach the adsorbed BSA, γ-globulins, and fibrinogen on the surface modified by the MPC polymer. A protein analysis kit (micro BCA protein assay kit, #23235; Thermo Fisher Scientific Inc., IL, USA) based on the BCA method was used to determine the BSA concentration in the SDS solution, and the amount of BSA, γ-globulins, and fibrinogen adsorbed on the surface modified by the MPC polymer was calculated.

2.9. Friction test and histological observation of articular cartilage

The coefficients of dynamic friction between the pins fabricated from articular cartilage and the surface-modified Co–Cr–Mo plates were measured by using a pin-on-plate machine (Tribostation 32; Shinto Scientific Co., Ltd., Tokyo, Japan). The friction tests were performed at room temperature and 37 °C with various loads in the range from 0.49 to 9.80 N, sliding distance of 25 mm, and frequency of 1 Hz for a maximum of 5×10^3 cycles [21]. Pure water, mixture of 25 vol% bovine serum (BS), 20 mM/L of ethylene diamine tetraacetic acid (EDTA), 0.1 mass% sodium azide, and the BS mixture containing 0.02 mass% MPC polymer (PMB30 (Mw = 5.0×10^4), PMSi90 (Mw = 9.8×10^4), and PMPC (Mw = 1.0×10^5)) were used as a lubricant each. Subsequently, five replicate measurements were performed for each sample, and the average values were regarded as the coefficients of dynamic friction. After 100 cycles of friction tests, the plate samples were FM-observed. Then, after 5×10^3 cycles friction test, articular cartilage pins against the untreated Co–Cr–Mo and PMPC-grafted Co–Cr–Mo were fixed with 10% neutral buffered formalin for 3 d, then decalcified in KC-X solution (Falma Co., Tokyo, Japan) for 8 d, and then dehydrated in graded ethanol for histological observation. The decalcified cartilage specimens were embedded in paraffin (Tissue-prep; Fisher Scientific Corp., Fair Lawn, NJ, USA), and microsections were prepared and stained with hematoxylin (Real hematoxylin; Dako Co., Carpinteria, CA, USA) and eosin (Eosin yellowish; Kanto Chemical Co., Inc.) (H&E) as well as with Safranin O (Nacalai Tesque, Inc., Kyoto, Japan) and observed with a microscope (Eclipse E600; Nikon Corp., Tokyo, Japan) equipped with a CCD camera (DP72; Olympus Co., Tokyo, Japan).

2.10. PBS soaking test

The surface-modified Co–Cr–Mo samples ($10 \times 10 \times 1$ mm^3 in size) were soaked in 50 mL of PBS. After soaking with 120 rpm shaking at 37 °C for 1, 4, 8, and 12 weeks, the samples removed from the PBS and were characterized by XPS analysis, water-contact angle measurement, and FM observation.

Table 1
Surface elemental composition ($n = 5$) and static-water contact angle ($n = 15$) of untreated, MPC polymer-coated and PMPC-grafted Co–Cr–Mo alloy.

Sample	Surface elemental composition (atom%)								Contact angle (deg)
	C_{1s}	O_{1s}	N_{1s}	P_{2p}	Si_{2p}	Co_{2p}	Cr_{2p}	Mo_{3d}	
Co–Cr–Mo (untreated)	14.6	52.9	0.0	0.0	0.0	26.7	5.4	0.4	81.6
	(1.3)[a]	(2.7)	(0.0)	(0.0)	(0.0)	(1.5)	(0.4)	(0.0)	(4.8)
PMB30-adsorbed Co–Cr–Mo	70.6	24.1	2.3	3.0	0.0	0.0	0.0	0.0	95.8[b]
	(1.4)	(1.3)	(0.4)	(0.3)	(0.0)	(0.0)	(0.0)	(0.0)	(3.5)
PMSi90-immobilized Co–Cr–Mo	61.4	29.5	3.6	4.2	1.3	0.1	0.0	0.0	16.6[b]
	(0.9)	(0.7)	(0.4)	(0.1)	(0.4)	(0.2)	(0.0)	(0.0)	(2.4)
PMPC-grafted Co–Cr–Mo	61.7	28.0	5.0	5.3	0.1	0.0	0.0	0.0	23.5[b]
	(0.7)	(0.6)	(0.3)	(0.1)	(0.1)	(0.0)	(0.0)	(0.0)	(8.4)

[a] The standard deviations are shown in parentheses.
[b] Significant difference ($p < 0.001$) as compared to the untreated Co–Cr–Mo.

2.11. Statistical analysis

The results derived from each measurement in the water-contact angle measurement, friction test, and protein adsorption test were expressed as mean values ± standard deviation. The statistical significance ($p < 0.05$) was estimated by Student's *t*-test.

3. Results

Fig. 2 shows the FT-IR/ATR spectra of the surface-modified Co–Cr–Mo samples with various MPC polymers. Absorption peaks were newly observed for the surface-modified Co–Cr–Mo with MPC polymers. The peaks at 1720, 1550, and 1460 cm^{-1} are attributed to C = O and -CH_2- in the MPC polymer. The peaks at 1180, 1040, 700, and 630 cm^{-1} are attributed to the trimethoxysilane group in the MPSi unit [19]. The peaks at 1240, 1080, 970, and 920 cm^{-1} are attributed to the $-N^+(CH_3)_3$ and phosphate groups in the MPC unit [22]. The absorption peak intensities of the phosphate groups of the PMPC-grafted Co–Cr–Mo were the highest in the Co–Cr–Mo whose surface was modified by the MPC polymer.

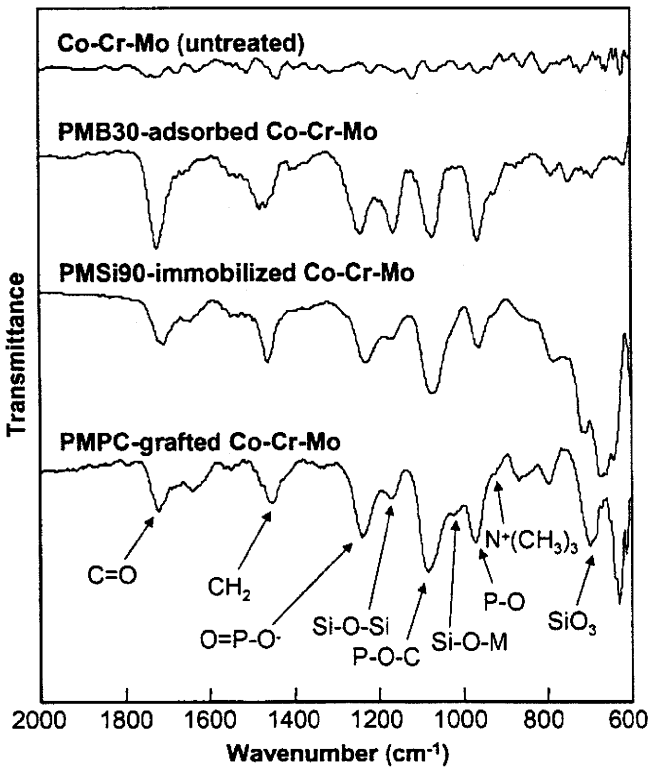

Fig. 2. FT-IR/ATR spectra of untreated Co–Cr–Mo, MPC polymer-coated Co–Cr–Mo, and PMPC grafted Co–Cr–Mo.

Table 1 summarizes the surface elemental composition and static-water contact angle of the surface-modified Co–Cr–Mo samples with various MPC polymers. The nitrogen (N) and phosphorous (P) contents in all the Co–Cr–Mo samples whose surfaces were modified by the MPC polymer were observed. The elemental compositions of both N and P in the surface-modified Co–Cr–Mo increased with an increase in the MPC composition in the polymer for surface modification. In particular, these values of N and P in the PMPC-grafted Co–Cr–Mo surface were 5.0 and 5.3 atom%, respectively, and were almost equivalent to the theoretical elemental composition (N = 5.3, P = 5.3 atom%) of PMPC. The static-water contact angle of the untreated Co–Cr–Mo was 81.6°, and this decreased markedly to approximately 20° (i.e., 16.6°–23.5°, $p < 0.001$) by the modifications with PMSi90 and PMPC.

Fig. 3 shows the cross-sectional TEM images of the surface-modified Co–Cr–Mo samples with various MPC polymers. For PMB30-adsorption, PMSi90-immobilization, and PMPC-grafting, a thickness of 50, 130, and 200 nm, respectively, of the MPC polymer layers was clearly observed on the surface of the Co–Cr–Mo substrate. No cracks due to poor adhesion and/or delamination were observed at the interface between the MPC polymer layer and Co–Cr–Mo substrate. These results indicate that each surface modification layer on the Co–Cr–Mo substrate is uniform and adheres closely, regardless of the binding conditions; the surface modification layers by PMB30-adsorption, PMSi90-immobilization, and PMPC-grafting combine with the substrate by physical adsorption and covalent bonds of Si–O–metal (M), respectively. However, in the PMB30-adsorbed Co–Cr–Mo, a bilayer structure for poor adhesion attributed to dipping twice was clearly observed on the surface modification layer. Further, in the PMB30-adsorbed and PMSi90-immobilized Co–Cr–Mo samples, a porous structure was clearly observed on the surface modification layer. This porous structure was also observed on the surface modification layer prepared by the slow-rate solvent evaporation method (approximately for 1 month at 4 °C, data not shown).

Fig. 4 shows the EDX spectra of the surface-modified Co–Cr–Mo samples with various MPC polymers. In spectra (b_{1-3}), (c_{1-3}), and (d_{1-3}) of the MPC polymer layers, a significant peak attributed to the P atom was observed at 2.0 keV. This peak is mainly attributed to the MPC units. Interestingly, this peak was clearly observed in spectra (b_2) and (c_2) of the porous part of the MPC polymer layer. In spectra (c_1) and (d_1) of the interface of the PMSi90-immobilization layer and the intermediate layer of the PMPC-grafted Co–Cr–Mo, peaks were observed at 0.5 and 1.7 keV. These peaks are attributed to the O and Si atoms in the interface/intermediate layer between the silane of the MPSi and the metal oxide of the Co–Cr–Mo.

Fig. 5 shows the amounts of BSA, γ-globulins, and fibrinogen adsorbed on the surface-modified Co–Cr–Mo samples with various

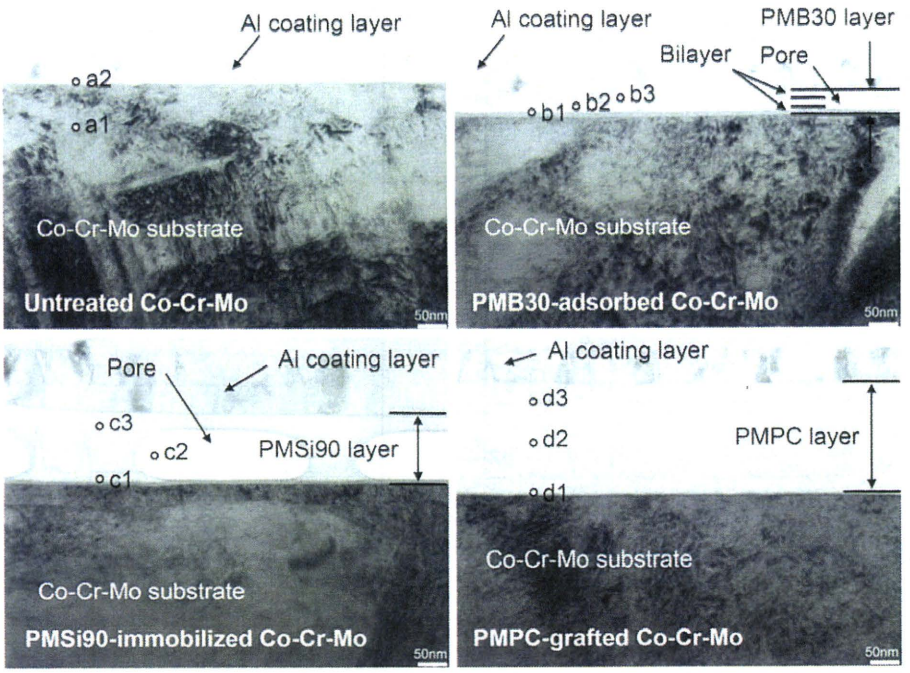

Fig. 3. Cross-sectional TEM images of the surface-modified Co–Cr–Mo with various MPC polymers. Aluminum coating layers (approximately 70–100 nm) for the preparation of TEM observation specimen are shown above the MPC polymer layer of the Co–Cr–Mo surface. Small open circles indicate EDX analysis points. Bar: 50 nm.

MPC polymers. The amount of each protein adsorbed on the Co–Cr–Mo surface modified by the MPC polymer was considerably lower ($p < 0.001$) than that on the untreated Co–Cr–Mo. These results imply that the surface modification by the MPC polymer results in good biocompatibility.

Fig. 6 shows the coefficients of dynamic friction of the sliding couples and articular cartilage pins sliding against the surface-modified Co–Cr–Mo plates with various MPC polymers. The PMB30-adsorbed and PMSi90-immobilized Co–Cr–Mo samples showed a slightly higher friction coefficient than the untreated Co–Cr–Mo sample in water at room temperature (not significantly different); in contrast, the MPC polymer-coated Co–Cr–Mo showed a lower friction coefficient than the untreated Co–Cr–Mo in BS mixture at 37 °C ($p < 0.05$). Further, the friction coefficient of the PMPC-grafted Co–Cr–Mo decreased drastically compared with untreated Co–Cr–Mo ($p < 0.001$) and reached approximately <0.010 in both lubricant conditions, i.e., water at room temperature and the BS mixture at 37 °C; moreover, it remained almost steady. The friction coefficients of all MPC polymer-containing BS mixtures were drastically lower as compared with that of non-additive BS mixture (Fig. 6).

Fig. 7 shows the coefficients of dynamic friction of the untreated Co–Cr–Mo and PMPC-grafted Co–Cr–Mo samples as a function of the loads. At both 10 and 100 cycles, the PMPC-grafted Co–Cr–Mo sample showed a remarkably low friction coefficient of approximately 0.019 at a load of 0.49 N; this value decreased gradually and reached approximately <0.010 at a load of 9.80 N. Similarly, the friction coefficients of the untreated Co–Cr–Mo sample in the initial 10 cycles decreased gradually from 0.188 to 0.045. However, this value of the untreated Co–Cr–Mo at 100 cycles decreased to 0.082 up to loads of 1.96 N; it then gradually increased with an increase in the loads. Fig. 7B shows the friction coefficients of the untreated Co–Cr–Mo and PMPC-grafted Co–Cr–Mo samples as a function of the test durations. It was observed that the friction coefficient was significantly lower in the PMPC-grafted Co–Cr–Mo sample than in the untreated Co–Cr–Mo one. This value was almost constant throughout the 5×10^3 cycles of the friction test.

Fig. 8 shows the histological findings of the articular cartilage pins after 5×10^3 cycles of friction tests. In the cartilage against the untreated Co–Cr–Mo, the cartilage layer of the worn surface became thicker as compared with the surrounding articular cartilage of the unworn surface. In contrast, in the cartilage against the PMPC-grafted Co–Cr–Mo, the layer of the worn surface did not differ considerably from that of the unworn surface.

Fig. 9 shows the time course of the surface modification layer of the untreated, MPC polymer-coated, and PMPC-grafted Co–Cr–Mo samples during PBS soaking. The elemental compositions of both N and P in the untreated, PMB30-adsorbed, and PMPC-grafted Co–Cr–Mo samples were almost constant throughout the 12 weeks of PBS soaking. In contrast, in the PMSi90-immobilized Co–Cr–Mo sample, these values decreased gradually with the PBS-soaking duration. Similarly, the static-water contact angle of untreated, PMB30-adsorbed, and PMPC-grafted Co–Cr–Mo samples were almost constant throughout PBS soaking, whereas the values in PMSi90-immobilized Co–Cr–Mo increased gradually.

Fig. 10 shows FM images of the surface-modified Co–Cr–Mo samples with various MPC polymers before and after friction tests/PBS-soaking tests. After 100 cycles of friction tests, the MPC polymer layer was removed from the PMB30-adsorbed and PMSi90-immobilized Co–Cr–Mo sliding surfaces; in contrast, most of the PMPC-grafted Co–Cr–Mo sliding surface was covered by the PMPC layer. After 12 weeks of PBS-soaking tests, most of the MPSi90 layer was removed from the Co–Cr–Mo surface, while most of the PMB30-adsorbed and PMPC-grafted Co–Cr–Mo surface was covered stably by the MPC polymer layer.

4. Discussion

In the hemi-arthroplasty, the highly lubricious surface by a "mild treatment" with soft materials was requested with aim of preserving the degradation of the articular cartilage. In this study, we have prepared various surface modification layers formed on the Co–Cr–Mo surface by MPC polymer coating or photoinduced radical polymerization of MPC to form PMPC graft chains for

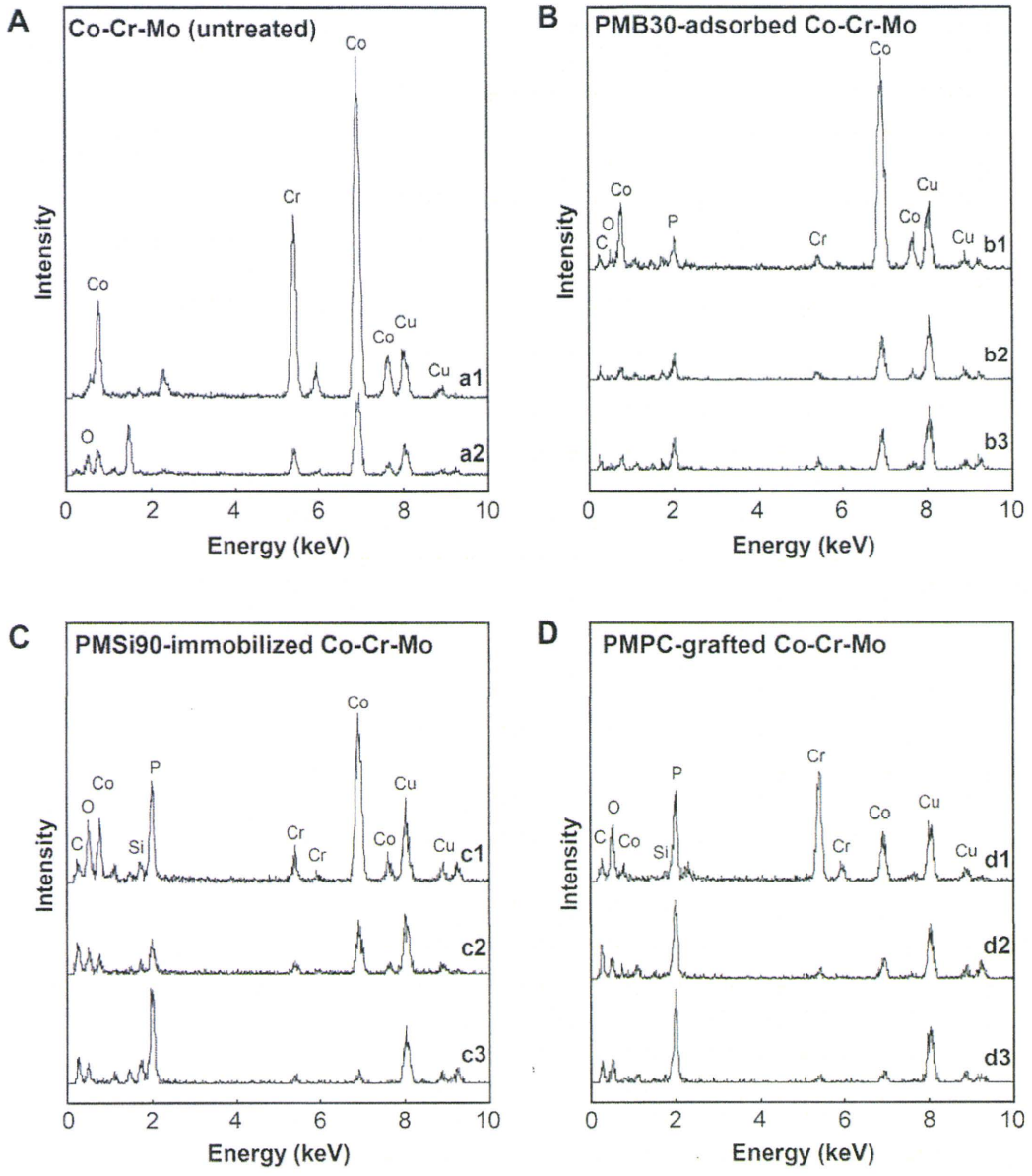

Fig. 4. EDX spectra of the untreated Co–Cr–Mo, MPC polymer-coated Co–Cr–Mo, and PMPC-grafted Co–Cr–Mo. The spectra were analyzed on the cross-section (small open circles in Fig. 3) of the untreated Co–Cr–Mo, MPC polymer-coated Co–Cr–Mo, and PMPC-grafted Co–Cr–Mo.

improving lubrication and preventing the degradation of acetabular cartilage. Here, we discuss the structures and stabilities of the surface modification layers of the MPC polymer and the effects of these characteristics on the retention of articular cartilage in hemiarthroplasty.

To ensure the *in vivo* long-term stability of the MPC modified layer on the Co–Cr–Mo surface, it is necessary to create strong covalent bonding between the Co–Cr–Mo substrate and the MPC polymer. Organosilanes have already been known as surface coupling agents that enhance bonding between a metal or a metal oxide surface and an organic resin such as dental resin; moreover, they can strongly bind metals to resins in dental implants [23]. Organic silanes or silane coupling agents comprise at least a hydrolyzable alkoxysilyl or chlorosilyl group and an organofunctional group. The agents are effective for introducing organofunctional groups into the siloxane network polymer. The organofunctional group in the silane could be useful for improving bonding with the organic overlayer. MPSi binds to the Co–Cr–Mo substrate by a condensation reaction in two steps; in the first step, MPSi is hydrolyzed (activated) and in the second step, the hydrolyzed silane molecule binds to the surface by an Si–O–M bond, forming branched hydrophobic siloxane bonds, i.e., Si–O–Si. The hydrolyzed silane molecule has three –OH groups that can react with the –OH groups of the surface metallic oxide layer to form siloxane bonds covalently. The peaks at 1180 and 1040 cm^{-1} in the FT-IR/ATR spectrum of the PMSi90-immobilized and PMPC-grafted Co–Cr–Mo surfaces were attributed to Si–O–Si and Si–O–M, respectively (Fig. 2).

However, several previous studies have reported that a silane coating has low water resistance due to hydrolysis of the siloxane bond and desorption of the physisorbed silane [24]. In fact, the PMSi90-immobilization layer was removed from the Co–Cr–Mo surface after 12 weeks of PBS soaking (Figs. 9 and 10). Zhang, et al. and others have reported that the water stability of Si–O–M could be improved by employing the following factors: (1) an induction of bridged silane coupling agents, when hydrolyzed, contain two or more $-Si(OH)_3$, (2) the hydrophobic alkyl moieties that limit the contact with water, and (3) an increase in the thickness of the

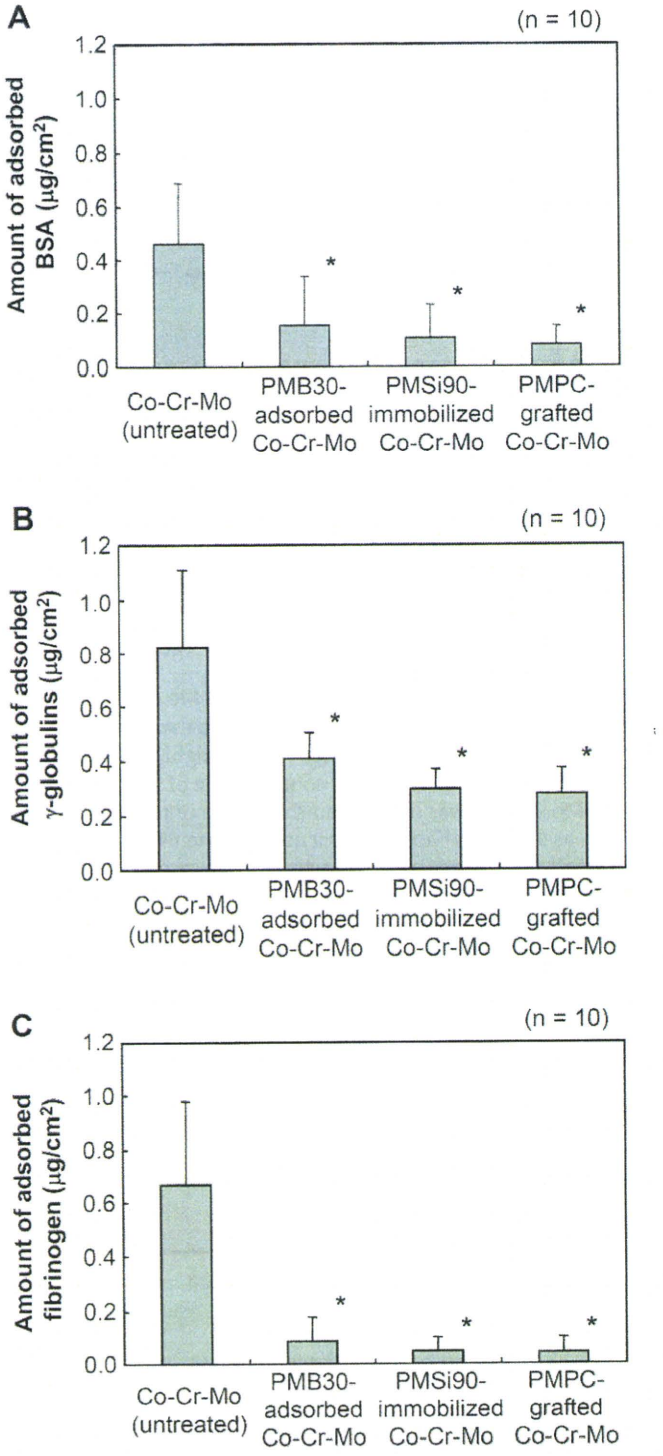

Fig. 5. Amounts of (A) BSA, (B) γ-globulins, and (C) fibrinogen adsorbed on the surfaces of the untreated Co–Cr–Mo, MPC polymer-coated Co–Cr–Mo, and PMPC-grafted Co–Cr–Mo. Bar: Standard deviations. *: Significant difference ($p < 0.001$) as compared to the untreated Co–Cr–Mo.

surface oxide layer [25]. Therefore, it was considered that the MPSi intermediate layer with a bridge of three methoxysilane groups with MPSi unit composition of 100% (MPSi unit of PMSi90 composition was 10% only) was essential in PMPC-grafted Co–Cr–Mo. Additionally, a functional methacrylate and pretreatment (nitric acid treatment and O_2 plasma treatment) for the Co–Cr–Mo surface were used. As shown in Figs. 9 and 10, the high stability of

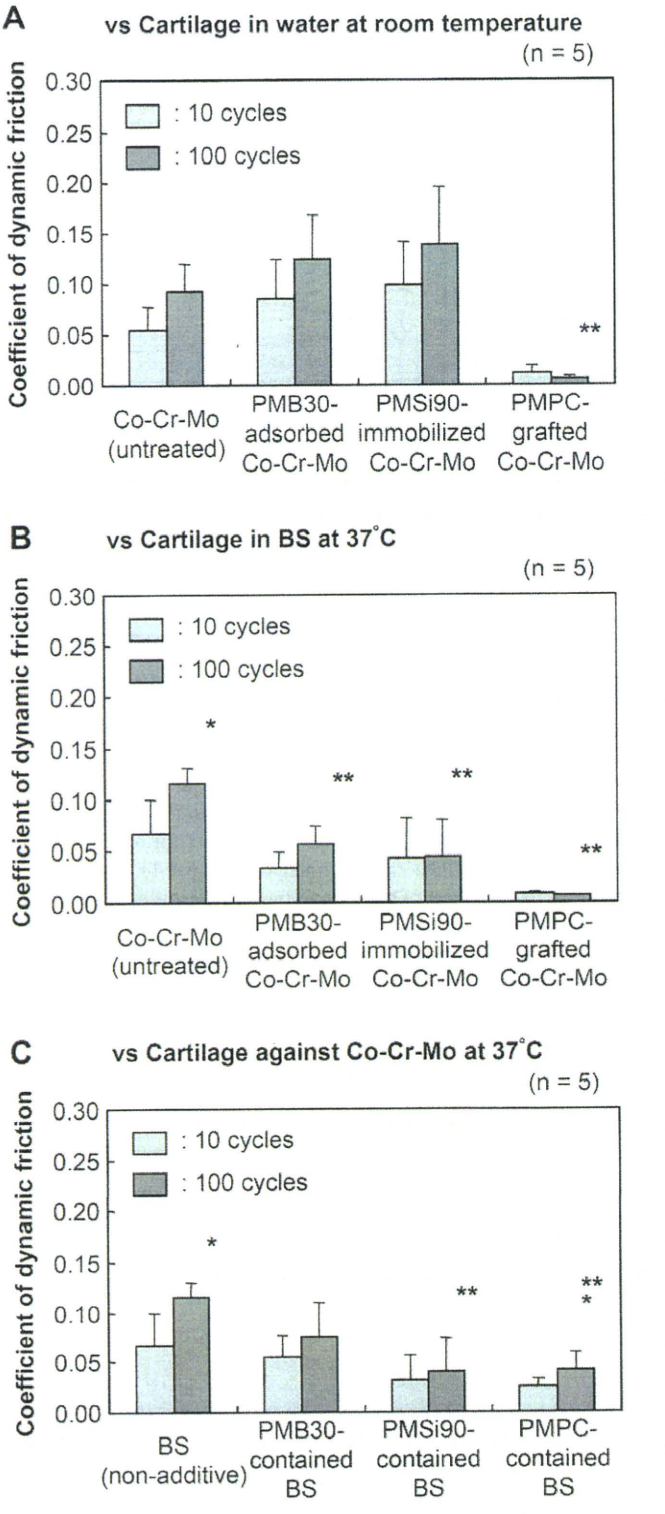

Fig. 6. Coefficients of dynamic friction of the untreated, MPC polymer-coated, and PMPC-grafted Co–Cr–Mo in the pin-on-plate friction test with various lubrication conditions. (A) Against cartilage pin with water at room temperature, (B) against cartilage pin with BS lubricant at 37 °C, (C) untreated Co–Cr–Mo plate against cartilage pin with BS lubricant with MPC polymer as additive at 37 °C. Bar: Standard deviations. *: *t*-test, significant difference ($p < 0.05$) as compared to the coefficients of dynamic friction at 10 cycles, and **: *t*-test, significant difference ($p < 0.05$) as compared to the untreated Co–Cr–Mo plate at 100 cycles.

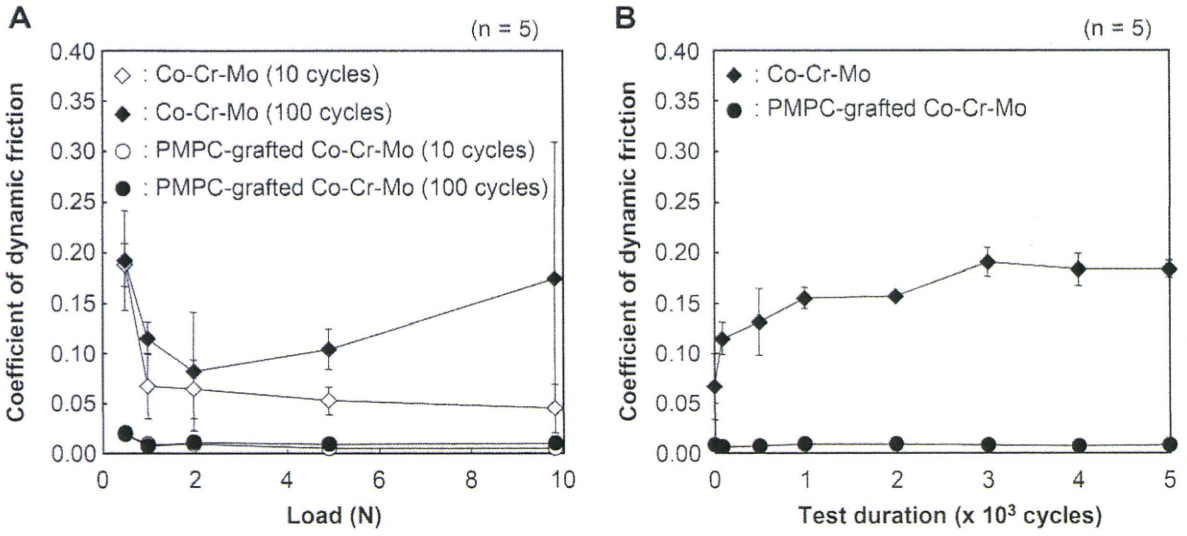

Fig. 7. Coefficients of dynamic friction of the untreated and PMPC-grafted Co–Cr–Mo in the pin-on-plate friction test. (A) Coefficients of dynamic friction of the untreated and PMPC-grafted Co–Cr–Mo against cartilage pin as a function of loads in the pin-on-plate friction test with BS lubricant at 37 °C. (B) Time course of coefficients of dynamic friction of the untreated and PMPC-grafted Co–Cr–Mo against the cartilage pin during 5×10^3 cycles of loading with 0.98 N in the pin-on-plate friction test with BS lubricant at 37 °C. Bar: Standard deviations.

the PMPC-grafted layer was confirmed throughout 12 weeks of PBS soaking.

On the other hand, the high stability of the PMB30-adsorbed layer was also confirmed throughout 12 weeks of PBS soaking. As shown in Table 1, the static-water contact angle of the PMB30-adsorbed Co–Cr–Mo was 95.8°. Sibarani et al. reported that the PMB30-adsorbed polymer surfaces showed high advancing (approximately 100°) and low receding (approximately 20°) contact angles: PMB30 cannot be hydrated easily due to the low MPC unit composition of the copolymer [10]. However, as shown in Fig. 5, the PMB30-adsorbed Co–Cr–Mo surface, which could form a phosphorylcholine-enriched surface after equilibrating for 1 h, showed excellent biocompatibility as an anti-protein adsorption surface. Hence, the PMB30-adsorbed layer has been observed to be stable (insoluble and attachable *in vivo* condition) and useful on several medical devices [14,15].

In Figs. 6 and 7, the PMPC-grafted Co–Cr–Mo surface shows an extremely low friction coefficient as compared to that of the untreated Co–Cr–Mo surface. Since MPC is highly hydrophilic and PMPC is water soluble, the water contact angle of the PMPC-grafted Co–Cr–Mo surface was lower than that of the untreated Co–Cr–Mo surface, as shown in Table 1. Consequently, the PMPC-grafted layer successfully provided high lubricity in the form of "surface gel hydration lubrication" to the Co–Cr–Mo surface (Fig. 3). A previous study has reported that the hydrogel cartilage surface is assumed to have a brush-like structure: a part of the proteoglycan brush is bonded with the collagen network on the cartilage surface [26]. The bearing surface with PMPC is assumed to have a brush-like structure similar to that of articular cartilage. Cartilage/PMPC-grafted Co–Cr–Mo bearing couples can therefore be regarded to be mimicking natural joint cartilage *in vivo*. The friction coefficient of cartilage/cartilage was reported to be approximately 0.01–0.02

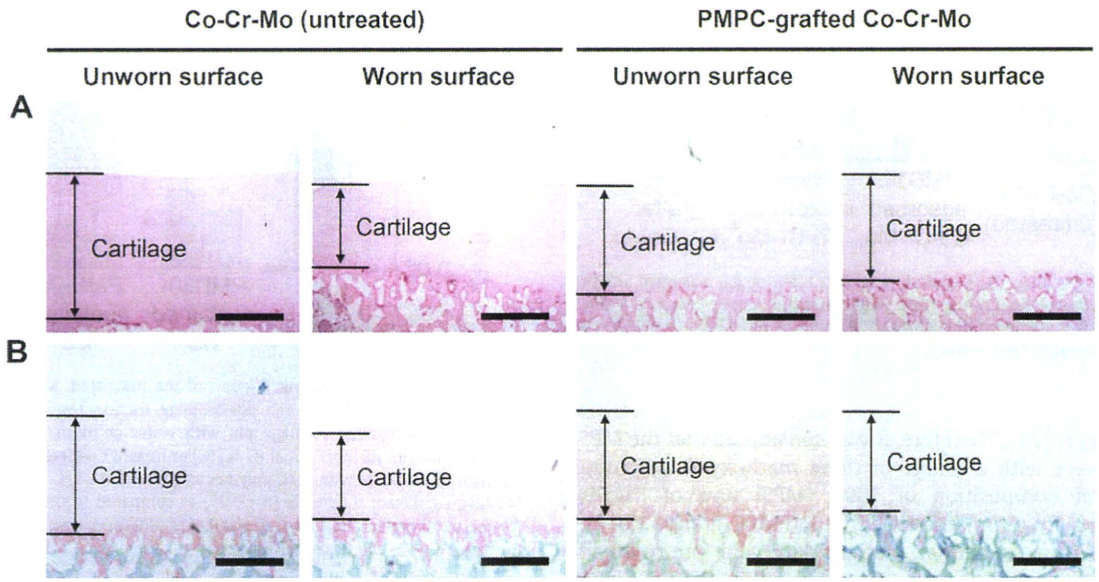

Fig. 8. Histological findings of the articular cartilage pins after 5×10^3 cycles of friction tests. (A) H&E stained, and (B) safranin-O stained. Bar; 500 μm.

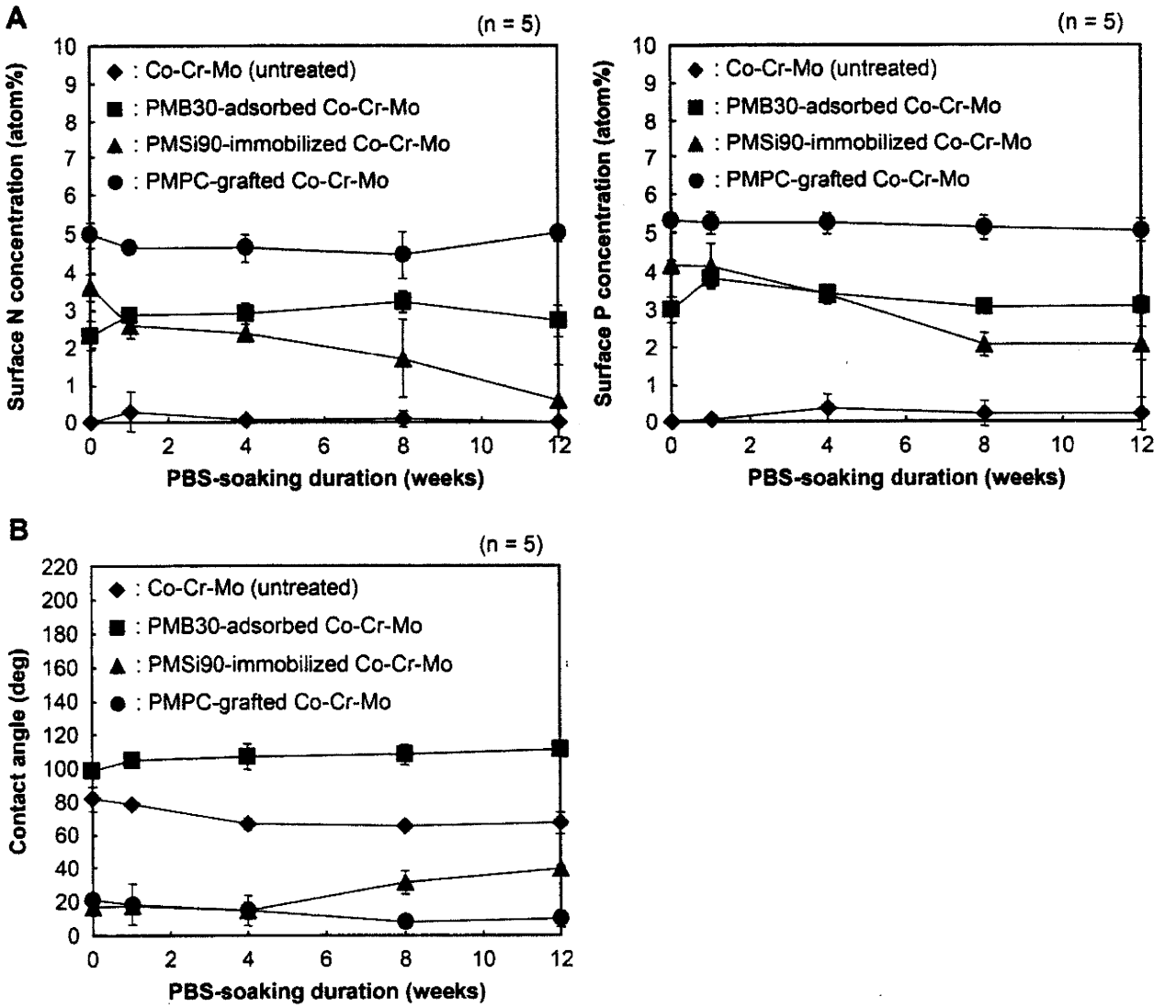

Fig. 9. Time course of the surface-modification layer of the untreated, MPC polymer-coated and PMPC-grafted Co–Cr–Mo during PBS soaking with 120 rpm shaking at 37 °C. (A) Surface N and P concentrations by XPS, and (B) static-water contact angle. Bar: Standard deviations.

[27,28]. In this study, it was found that the cartilage/PMPC-grafted Co–Cr–Mo interface mimicking a natural joint showed low friction (friction coefficient was <0.01), i.e., as low as that of cartilage/cartilage interface. Hence, it was considered that the PMPC-grafted Co–Cr–Mo surface is well suited for application on the artificial femoral head that would chafe against articulating cartilage. We expect that hemi-arthroplasty with a PMPC-grafted Co–Cr–Mo femoral head will be a promising option that preserves acetabular cartilage and extends the duration before total hip arthroplasty (THA) in young patients. Moreover, we consider that these effects would occur continuously. In Fig. 7B, the friction coefficient shows a test duration-dependent response for articular cartilage against the untreated Co–Cr–Mo sample due to the continued loading of the cartilage tissue and the ensuing loss of fluid-film formation (or rehydration). It was thought that the thickness of the cartilage tissue atrophied due to the fairly poor access of the cartilage tissue to water (Fig. 8). Decreased water content often leads to the degradation of cartilage function. Although cartilage tissues are able to produce matrix components throughout life, i.e., carry out regeneration, their production cannot keep pace with the repair requirements after acute damage to articular cartilage; such damages limit the longevity of the artificial femoral head and its stability after hemi-arthroplasty. In contrast, in articular cartilage against the PMPC-grafted Co–Cr–Mo sample, the friction coefficient remained at a steady low value due to the rehydration of the continuously loaded cartilage tissue, and the articular cartilage surface was preserved.

In Fig. 6A, the PMB30-adsorbed and PMSi90-immobilized Co–Cr–Mo samples show a slightly higher friction coefficient than the untreated Co–Cr–Mo sample in water at room temperature. Some pores in the PMB30 and PMSi90 layers on the Co–Cr–Mo surface could be observed (Fig. 3); these may have occurred due to the low density of the material because physical adsorption or chemical immobilization of the polymer was used as the surface modification method. Therefore, it is assumed that a sliding couple with cartilage and low-density MPC polymer layer may cause high friction by stick-slip motion with interpenetration [18]. Furthermore, the MPC polymer-coated Co–Cr–Mo showed a lower friction coefficient than the untreated Co–Cr–Mo in BS mixture at 37 °C (Fig. 6B). It was thought that the interpenetration of cartilage and low-density MPC polymer layer was blocked by the protein of BS presented between the interfaces. In contrast, the friction coefficient of the PMPC-grafted Co–Cr–Mo sample was drastically as compared with that of the untreated Co–Cr–Mo sample; the degree

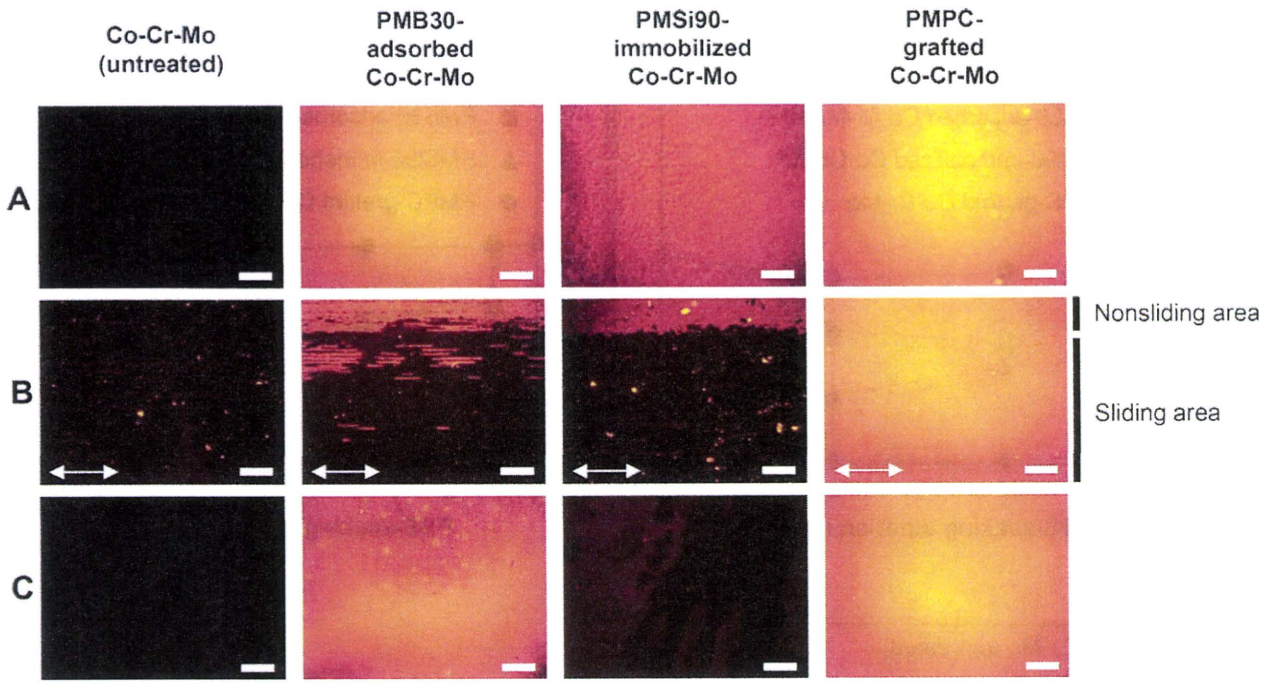

Fig. 10. FM images of the untreated Co–Cr–Mo, MPC polymer-coated Co–Cr–Mo, and PMPC-grafted Co–Cr–Mo surfaces. FM images of the surface before tests (A), after 100 cycles of friction tests with BS lubricant (B), and after 12 weeks of PBS-soaking tests (C). Bar; 200 μm. Arrow; Sliding direction of friction test.

of reduction in the coefficient was 93%. PMPC-grafted Co–Cr–Mo might have a high density because the polymerization method used was surface-initiated graft polymerization, termed as the "grafting from" method [19,29]. A sliding couple with cartilage tissue and high-density PMPC layer fabricated by the "grafting from" method may be responsible for low friction, such as that in the case of "super-lubricity," because of resistance to interpenetration by volume effects resulting from the mobility of hydrophilic macromolecules of cartilage tissue and the PMPC-grafted layer [30–32].

As shown in Fig. 7A, the friction coefficients of the articular cartilage against the untreated and PMPC-grafted Co–Cr–Mo samples decreased with an increasing load in the initial 10 cycles. The elastic articular cartilage tissue and PMPC-grafted layer was slightly deformed by the loads; the low friction coefficient might occur in order to increase the contact area of the fluid film's concave surface. However, the friction coefficient of the articular cartilage against the untreated Co–Cr–Mo at 100 cycles decreased to 0.082 up to loads of 1.96 N; a further increase in loads up to 9.8 N resulted in elevated friction coefficients. Under a high load, water exudes slowly from the articular cartilage with sliding [27]. As the result of water loss, the thickness of the surface layer and/or fluid film reduces, and the water content of the surface-hydration layer decreases. Consequently, the degree of adhesion of articular cartilage to the Co–Cr–Mo surface increases due to a lack of rehydration and because of the increase in frictional force. In contrast, the PMPC-grafted Co–Cr–Mo sample at 100 cycles showed a remarkably low friction coefficient that reached approximately <0.010 at a load of 9.80 N. We consider that this result implies that the rehydration and hydrodynamic lubrication mechanism of the articular cartilage is supported by the hydrated PMPC-grafted layer, similar to the interface between cartilage/cartilage of the natural joint.

The friction coefficients of cartilage/untreated Co–Cr–Mo interface with all MPC polymer-containing BS mixtures as a lubricant were drastically lower as compared with that with the non-additive BS mixture (Fig. 6C). Synovial fluid as a whole, and all its components such as hyaluronic acid, glycoprotein (mainly lubricin), and surface-active phospholipids, have been proposed as lubricants responsible for boundary lubrication in the natural joint [33]. Similarly, it is considered that the additives of MPC polymer would play the role akin to synovial phospholipids for boundary lubrication, and the adsorption of the MPC polymer to the sliding surface could prevent direct contact between the cartilage and the untreated Co–Cr–Mo and hence decrease the frictional force between them. However, in the case of additives, the lubricity may change depending on the ambient *in vitro* and *in vivo* conditions, because the additives probably diffuse to synovial fluid *in vivo*.

The amounts of the representative protein, BSA, γ-globulins, and fibrinogen, adsorbed on the modified Co–Cr–Mo surface with the MPC polymer were significantly low, these reached to 7%–50% of that of the untreated surface, as shown in Fig. 5. It is hypothesized that the mechanism underlying protein adsorption resistivity of a surface modified by the MPC polymer is based on the water structure resulting from the interactions between water molecules and phosphorylcholine groups [34]. The large amount of free water around the phosphorylcholine group is considered to detach proteins easily and prevent conformational changes in the adsorbed proteins even when the proteins attached to the surface [3,34]. The reduction in protein adsorption is also considered to be caused by the presence of a hydrated layer around the phosphorylcholine group [35]. The latter consideration is consistent with the results of the water contact angle measurement, friction test, and TEM and FM observations of the Co–Cr–Mo samples whose surfaces were modified by the MPC polymer. It should be noted that the porous structure (low density) of the PMB30-adsorption and PMSi90-immobilization layer (in dry conditions) hardly affected the protein adsorption. Therefore, the Co–Cr–Mo sample whose surface is modified by the MPC polymer is expected to exhibit tissue and blood compatibility, i.e., biocompatibility, because previous studies have reported that the MPC polymer-modified surfaces exhibit *in vivo* biocompatibility [6–16].

5. Conclusions

In this study, we systematically investigated the surface properties of the various surface modification layers formed on the Co–Cr–Mo surface by the MPC polymer by dip coating or photoinduced radical grafting. We conclude that several important issues are involved in the long-term retention of the benefits of the MPC polymer used in artificial joints under variable and multidirectional loads, for example, strong bonding between the MPC polymer and the Co–Cr–Mo surface as also a high density of the MPC polymer. We suggest that the MPSi intermediate layer and photoinduced radical graft polymerization should be employed to create strong covalent bonding between the surface modification layer and Co–Cr–Mo substrate and to retain the high density of the polymer chains of that layer. The cartilage/PMPC-grafted Co–Cr–Mo interface, which mimicked a natural joint, showed an extremely low friction coefficient of <0.01, a value as low as that of a natural cartilage interface. We expect that the PMPC-grafted Co–Cr–Mo femoral head for hemi-arthroplasty will be a promising option for preserving acetabular cartilage and extending the duration before THA.

Acknowledgements

This study was supported by the Health and Welfare Research Grant for Translational Research (H17-005), Research on Medical Devices for Improving Impaired QOL (H20-004) from the Japanese Ministry of Health, Labour and Welfare. We thank Mr. Y. Yoshihara and Ms. Y. Nakao, Japan Medical Materials Corporation, for their excellent technical assistance.

Appendix

Figures with essential colour discrimination. Certain figures in this article, in particular Figures 8 and 10, are difficult to interpret in black and white. The full colour images can be found in the on-line version, at doi:10.1016/j.biomaterials.2009.09.083.

References

[1] Healy WL, Lemos DW, Appleby D, Lucchesi CA, Saleh KJ. Displaced femoral neck fractures in the elderly: outcomes and cost effectiveness. Clin Orthop Relat Res 2001;383:229–42.
[2] Beaulé PE, Amstutz HC, Le Duff M, Dorey F. Surface arthroplasty for osteonecrosis of the hip: hemiresurfacing versus metal-on-metal hybrid resurfacing. J Arthroplasty 2004;19(8 Suppl. 3):54–8.
[3] Kyomoto M, Moro T, Miyaji F, Hashimoto M, Kawaguchi H, Takatori Y, et al. Effects of mobility/immobility of surface modification by 2-methacryloyloxyethyl phosphorylcholine polymer on the durability of polyethylene for artificial joints. J Biomed Mater Res A 2009;90(2):362–71.
[4] Kyomoto M, Moro T, Miyaji F, Hashimoto M, Kawaguchi H, Takatori Y, et al. Effect of 2-methacryloyloxyethyl phosphorylcholine concentration on photo-induced graft polymerization of polyethylene in reducing the wear of orthopaedic bearing surface. J Biomed Mater Res A 2008;86(2):439–47.
[5] Kyomoto M, Moro T, Miyaji F, Konno T, Hashimoto M, Kawaguchi H, et al. Enhanced wear resistance of orthopedic bearing due to the cross-linking of poly(MPC) graft chains induced by gamma-ray irradiation. J Biomed Mater Res B Appl Biomater 2008;84(2):320–7.
[6] Moro T, Takatori Y, Ishihara K, Konno T, Takigawa Y, Matsushita T, et al. Surface grafting of artificial joints with a biocompatible polymer for preventing periprosthetic osteolysis. Nature Mater 2004;3:829–37.
[7] Moro T, Takatori Y, Ishihara K, Nakamura K, Kawaguchi H. 2006 Frank Stinchfield Award: grafting of biocompatible polymer for longevity of artificial hip joints. Clin Orthop Relat Res 2006;453:58–63.
[8] Moro T, Kawaguchi H, Ishihara K, Kyomoto M, Karita T, Ito H, et al. Wear resistance of artificial hip joints with poly(2-methacryloyloxyethyl phosphorylcholine) grafted polyethylene: comparisons with the effect of polyethylene cross-linking and ceramic femoral heads. Biomaterials 2009;30(16):2995–3001.
[9] Kyomoto M, Ishihara K. Self-initiated surface graft polymerization of 2-methacryloyloxyethyl phosphorylcholine on poly(ether–ether–ketone) by photo-irradiation. ACS Appl Mater Interfaces 2009;1(3):537–42.
[10] Sibarani J, Takai M, Ishihara K. Surface modification on microfluidic devices with 2-methacryloyloxyethyl phosphorylcholine polymers for reducing unfavorable protein adsorption. Colloids Surf B Biointerfaces 2007;54(1):88–93.
[11] Ueda T, Oshida H, Kurita K, Ishihara K, Nakabayashi N. Preparation of 2-methacryloyloxyethyl phosphorylcholine copolymers with alkyl methacrylates and their blood compatibility. Polym J 1992;24(11):1259–69.
[12] Konno T, Ishihara K. Temporal and spatially controllable cell encapsulation using a water-soluble phospholipid polymer with phenylboronic acid moiety. Biomaterials 2007;28(10):1770–7.
[13] Xu Y, Takai M, Konno T, Ishihara K. Microfluidic flow control on charged phospholipid polymer interface. Lab Chip 2007;7(2):199–206.
[14] Snyder TA, Tsukui H, Kihara S, Akimoto T, Litwak KN, Kameneva MV, et al. Preclinical biocompatibility assessment of the EVAHEART ventricular assist device: coating comparison and platelet activation. J Biomed Mater Res A 2007;81(1):85–92.
[15] Ueda H, Watanabe J, Konno T, Takai M, Saito A, Ishihara K. Asymmetrically functional surface properties on biocompatible phospholipid polymer membrane for bioartificial kidney. J Biomed Mater Res A 2006;77(1):19–27.
[16] Kyomoto M, Moro T, Konno T, Takadama H, Yamawaki N, Kawaguchi H, et al. Enhanced wear resistance of modified cross-linked polyethylene by grafting with poly(2-methacryloyloxyethyl phosphorylcholine). J Biomed Mater Res A 2007;82(1):10–7.
[17] Ishihara K, Ueda T, Nakabayashi N. Preparation of phospholipid polymers and their properties as polymer hydrogel membranes. Polym J 1990;22(5):355–60.
[18] Kyomoto M, Iwasaki Y, Moro T, Konno T, Miyaji F, Kawaguchi H, et al. High lubricious surface of cobalt–chromium–molybdenum alloy prepared by grafting poly(2-methacryloyloxyethyl phosphorylcholine). Biomaterials 2007;28(20):3121–30.
[19] Kyomoto, M., Moro, T., Iwasaki, Y., Miyaji, F., Kawaguchi, H., Takatori, Y., et al. Superlubricious surface mimicking articular cartilage by grafting poly(2-methacryloyloxyethyl phosphorylcholine) on orthopaedic metal bearings. J Biomed Mater Res A, in press.
[20] Wang JH, Bartlett JD, Dunn AC, Small S, Willis SL, Driver MJ, et al. The use of rhodamine 6G and fluorescence microscopy in the evaluation of phospholipid-based polymeric biomaterials. J Microsc 2005;217(Pt 3):216–24.
[21] Arendt SA, Bailey SJ, editors. ASTM F732–00: standard test method for wear testing of polymeric materials used in total joint prostheses. Annual book of ASTM standards, vol. 13; 2004.
[22] Kyomoto M, Moro T, Konno T, Takadama H, Kawaguchi H, Takatori Y, et al. Effects of photo-induced graft polymerization of 2-methacryloyloxyethyl phosphorylcholine on physical properties of cross-linked polyethylene in artificial hip joints. J Mater Sci Mater Med 2007;18:1809–15.
[23] Yoshida K, Greener EH. Effects of coupling agents on mechanical properties of metal oxide-polymethacrylate composites. J Dent 1994;22:57–62.
[24] Matinlinna JP, Vallittu PK. Bonding of resin composites to etchable ceramic surfaces – an insight review of the chemical aspects on surface conditioning. J Oral Rehabil 2007;34(8):622–30.
[25] Zhang Z, Berns AE, Willbold S, Buitenhuis J. Synthesis of poly(ethylene glycol) (PEG)-grafted colloidal silica particles with improved stability in aqueous solvents. J Colloid Interface Sci 2007;310(2):446–55.
[26] Ishikawa Y, Hiratsuka K, Sasada T. Role of water in the lubrication of hydrogel. Wear 2006;261:500–4.
[27] Katta J, Jin Z, Ingham E, Fisher J. Biotribology of articular cartilage – a review of the recent advances. Med Eng Phys 2008;30(10):1349–63.
[28] Bell CJ, Ingham E, Fisher J. Influence of hyaluronic acid on the time-dependent friction response of articular cartilage under different conditions. Proc Inst Mech Eng [H] 2006;220(1):23–31.
[29] Matsuda T, Kaneko M, Ge S. Quasi-living surface graft polymerization with phosphorylcholine group(s) at the terminal end. Biomaterials 2003;24:4507–15.
[30] Raviv U, Glasson S, Kampf N, Gohy JF, Jérôme R, Klein J. Lubrication by charged polymers. Nature 2003;425:163–5.
[31] Chen M, Briscoe WH, Armes SP, Klein J. Lubrication at physiological pressures by polyzwitterionic brushes. Science 2009;323(5922):1698–701.
[32] Kobayashi M, Terayama Y, Hosaka N, Kaido M, Suzuki A, Yamada N, et al. Friction behavior of high-density poly(2-methacryloyloxyethyl phosphorylcholine) brush in aqueous media. Soft Matter 2007;2:740–6.
[33] Sawae Y, Yamamoto A, Murakami T. Influence of protein and lipid concentration of the test lubricant on the wear of ultra high molecular weight polyethylene. Tribol Int 2008;41(7):648–56.
[34] Goda T, Konno T, Takai M, Ishihara K. Photoinduced phospholipid polymer grafting on Parylene film: advanced lubrication and antibiofouling properties. Colloids Surf B Biointerfaces 2007;54(1):67–73.
[35] Hoshi T, Sawaguchi T, Konno T, Takai M, Ishihara K. Preparation of molecular dispersed polymer blend composed of polyethylene and poly(vinyl acetate) by in situ polymerization of vinyl acetate using supercritical carbon dioxide. Polymer 2007;48(6):1573–80.

///VSP///

Journal of Biomaterials Science 22 (2011) 77–89

Journal of BIOMATERIALS SCIENCE
brill.nl/jbs

Spontaneous Formation of a Hydrogel Composed of Water-Soluble Phospholipid Polymers Grafted with Enantiomeric Oligo(lactic acid) Chains

Kimiaki Takami [a,b,c], **Junji Watanabe** [d], **Madoka Takai** [b,d] **and Kazuhiko Ishihara** [a,b,c,d,*]

[a] Department of Bioengineering, The University of Tokyo. 7-3-1 Hongo, Bunkyo-ku, Tokyo 113-8656, Japan

[b] Center for NanoBio Integration, The University of Tokyo, 7-3-1 Hongo, Bunkyo-ku, Tokyo 113-8656, Japan

[c] Center for Medical System Innovation, The University of Tokyo, 7-3-1 Hongo, Bunkyo-ku, Tokyo 113-8656, Japan

[d] Department of Materials Engineering, The University of Tokyo, 7-3-1 Hongo, Bunkyo-ku, Tokyo 113-8656, Japan

Received 16 June 2009; accepted 7 November 2009

Abstract

We designed and synthesized water-soluble biocompatible and biodegradable polymers composed of 2-methacryroyloxyethyl phosphorylcholine and oligo(L- or D-lactic acid) macromonomers to develop an injectable hydrogel matrix. Aqueous solutions containing the polymers with oligo(L-lactic acid) (OLLA) and oligo(D-lactic acid) (ODLA) chains underwent spontaneous gelation when mixed together. This was due to the formation of a stereocomplex between the OLLA and ODLA side-chains, which act as cross-linking components in the hydrogel. Therefore, the hydrogel could be re-dissolved in a buffer solution by hydrolysis of the oligo(lactic acid) chains. We obtained an injectable, biocompatible and degradable hydrogel, and we anticipate that it will be used in applications involving the controlled release of bioactive molecules and cell-based tissue engineering.

Keywords

Injectable hydrogel, phospholipid polymer, poly(lactic acid), biodegradation, stereocomplex formation

1. Introduction

In general, artificial materials are recognized as a foreign body in living organisms because of insufficient biocompatibility. When implanted into soft tissues, they induce a series of inflammatory reactions and are finally encapsulated by the tissues.

* To whom correspondence should be addressed. E-mail: ishihara@mpc.t.u-tokyo.ac.jp

DOI:10.1163/092050609X12578498967995

Thus, they do not interact favorably with the surrounding tissues to form a bond. Consequently, common artificial materials cannot be used in therapies based on tissue regeneration. Moreover, when these materials come into contact with blood, they rapidly induce thrombus formation. At present, it is desirable to use medical devices for the treatment of diseases, but these devices should combine pretreatment with drugs such as anti-inflammatory reagents and anticoagulants. Thus, the materials used in living organisms should have excellent biocompatibility. In addition, the presence of artificial materials in living organisms can result in persistent inflammation and infection; moreover, cytotoxic substances may be generated and released by the unexpected degradation of the artificial material and prevent tissue healing. Therefore, it is essential to ensure that the materials used in living organisms are biodegradable. In terms of clinical application, the use of surgical methods for implantation results in greater patient pain. However, materials that cause spontaneous gelation in living organisms enable percutaneous implantation. Hydrogels are suitable for use in implantable devices [1]. Because their mechanical properties are similar to those of living tissue, interaction between the material and cells or body fluid may be more favorable and blood vessels can easily penetrate the hydrogel matrices. Hydrogels that cause spontaneous gelation are preferable for use as biomaterials in minimally invasive surgery [2, 3], and it is desirable to develop such materials that possess the properties of spontaneous gelation and biodegradability. The purpose of this study is to develop a hydrogel that undergoes spontaneous gelation. The hydrogel must also possess blood compatibility and absorbability for use as a base material in various applications such as scaffolds for tissue engineering, drug reservoirs for drug-delivery systems, and biomedical glue and anti-adhesive materials for use in surgical treatments. In this study, we investigated the design of materials for these medical applications.

It is well known that the blending of poly(L-lactic acid) (PLLA) and poly(D-lactic acid) (PDLA) results in the formation of a eutectic called a stereocomplex [4–8]. Block co-polymers composed of poly(ethylene glycol) (PEG) and PLLA or PDLA were reported to be injectable hydrogels based on stereocomplex formation. Li *et al.* reported gelation by the formation of a stereocomplex between the PLLA and PDLA segments in the block co-polymers in an aqueous medium. These polymer gels contained water and underwent hydrolysis and absorption under physiological conditions [9, 10]. In previous studies, we reported on the spontaneous formation of a polymer hydrogel from 2-methacryloyloxyethyl phosphorylcholine (MPC) and *n*-butyl methacrylate (BMA) units and poly(lactic acid) chains (PMBLA) [11, 12]. From a chloroform solution containing MPC polymers with both PLLA chains and PDLA chains, the polymer gel was formed as a stereocomplex with cross-linking components. After the solvent was removed, the gel could be used for cell culture due to its highly porous structure, with cells easily able to penetrate it.

MPC polymers containing BMA units are highly biocompatible and cytocompatible and have been used as coating materials on implantable medical devices

[13–21]. Since the gel can be dissociated by hydrolysis of poly(lactic acid) chains as cross-linking points and become water-soluble, it can be safely removed from the living organism.

In the case of a poly(lactic acid)/PEG block co-polymer hydrogel system, it is difficult to achieve functional control due to difficulties encountered in hydrogel preparation [22, 23]. On the other hand, the properties and functions of PMBLA can be easily regulated through simple random co-polymerization with changes in both the composition and the chemical structure of the monomer units.

In this study, in order to enhance the safety of hydrogel materials, we synthesized a novel water-soluble MPC polymer (PMLA) composed of MPC units along with oligo(lactic acid) macromonomer units as a cross-linking functional group. We used oligo(L-lactic acid) (OLLA) and oligo(D-lactic acid) (ODLA) macromonomers to synthesize the hydrogel through the formation of a stereocomplex between these OLLA and ODLA chains. The gelation time could be controlled by the oligo(lactic acid) concentration in the solution, and we investigated a range of PMLA solutions that form hydrogels in living tissue following percutaneous injection *via* a syringe. We propose an implantable hydrogel system for use in *in vivo* tissue-engineering applications to facilitate the development of cell-based medical treatments.

2. Materials and Methods

2.1. Materials

MPC was synthesized by a previously reported method and obtained from NOF (Tokyo, Japan) [24, 25]. L-Lactide and D-lactide (Purac, Gorinchem, The Netherlands) were recrystallized from ethyl acetate. 2, 2′-Azobisisobutylnitrile (AIBN; Wako Chemicals, Osaka, Japan) was recrystallized from methanol. Tin(II) 2-ethylhexanoate (Wako Chemicals), 2-hydroxyethyl methacrylate (HEMA; Wako Chemicals), and other solvents were obtained as extra pure reagents and used without further purification. *p*-Xylene N,N′-diethyldithiocarbamate (XDC) was synthesized in accordance with the procedure described in a previous paper [26]. Bovine serum albumin and fluoresceine isothiocianate (FITC)-labeled BSA were obtained from Sigma-Aldrich (St Louis, MO, USA) and were used without further purification.

2.2. Synthesis of Oligo(lactic acid) Macromonomers

OLLA and ODLA macromonomers were synthesized (Scheme 1) by the method described in an earlier study [27]. The desired amounts of L-lactide and D-lactide were introduced into round bottom flasks and tin(II)2-ethylhexanoate was also added to each flask. Each flask was sealed by a three-neck cock. The insides of the flasks were evacuated by a vacuum pump operating at 10 mmHg for 1 h. Argon gas was blown into the flasks to replace the atmosphere. Then, HEMA was poured into each flask and polymerization was carried out for 6 h at 120°C.

The products were dissolved in 20 ml dichloromethane and precipitated in a 300-ml mixture of 2-propanol/hexane (1:1, v/v) for purification. The precipitates were washed in the same solvent and the final suspension was centrifuged (1×10^4 rpm, 10 min). After removal of the supernatant and vacuum drying, the OLLA and ODLA macromonomers were obtained as a white powder.

2.3. Synthesis of PMLA

Desired amounts of the OLLA macromonomer or the ODLA macromonomer and AIBN were placed in round bottom flasks and dissolved in 25 ml dioxane. MPC dissolved in 25 ml ethanol was added to the solution. The flasks were sealed after argon gas bubbling, and co-polymerization was carried out at 60°C for 24 h. After co-polymerization, the products were evaporated and poured into a 300-ml mixture of hexane/chloroform (9:1, v/v). The precipitate was filtered and dried *in vacuo* for 24 h. The polymers containing OLLA and ODLA chains and prepared using AIBN were designated as A-PMLLA and A-PMDLA, respectively.

Photoinduced living radical polymerization of MPC and oligo(lactic acid) macromonomers was carried out as follows (Scheme 2). Desired amounts of the OLLA macromonomer or ODLA macromonomer and XDC were placed in a glass tube and dissolved in 50 ml dioxane. MPC dissolved in ethanol was added to the solutions. The tube was sealed after argon gas had been bubbled through it for 5 min to eliminate oxygen in the solution, and the sealed tube was irradiated at 25°C for 6 h using an ultra-high-pressure mercury lamp (UVL-400HB, Riko, Chiba, Japan). A wavelength of 360 nm was selected using a glass color filter (Riko U-360). Af-

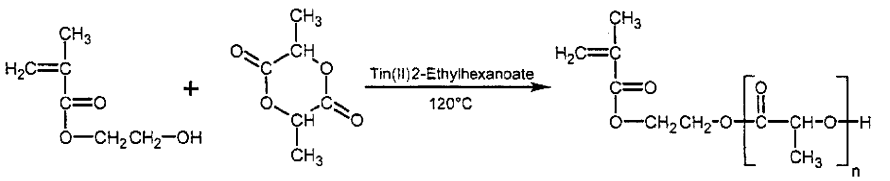

Scheme 1. Synthetic route of oligo(lactic acid) macromonomer.

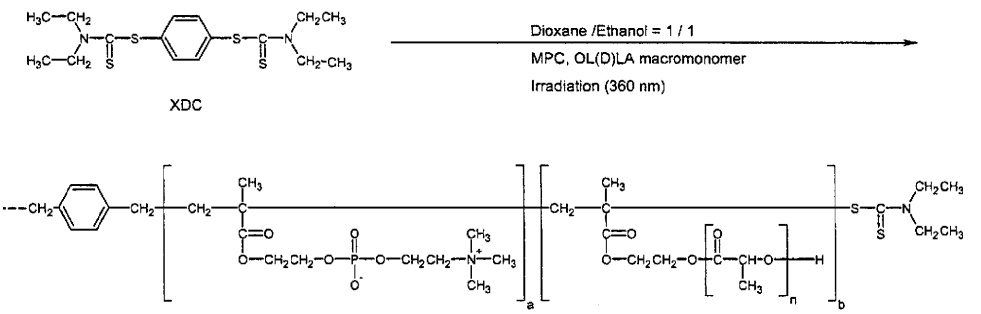

Scheme 2. Synthetic route of water-soluble MPC polymer grafted with oligo(lactic acid) side-chains by living radical polymerization using XDC as the iniferter.

ter polymerization, the reaction mixtures were poured into a 300-ml mixture of hexane/chloroform (9:1, v/v). The precipitate was filtered and dried *in vacuo* for 24 h. The polymers containing OLLA and ODLA chains and prepared using XDC were designated as X-PMLLA and X-PMDLA, respectively.

2.4. Analysis of Polymer Chemical Structure

The chemical structures of the oligo(lactic acid) macromonomers were determined by ^{1}H-NMR. For the NMR measurements, a 6-mg each of the macromonomers and polymers was dissolved in 700 μl $CDCl_3$ or C_2D_5OD. Chemical shifts were measured using a JNM-AL300 (Jeol, Tokyo, Japan) at 20°C. The degree of polymerization was calculated from the peak area ratio of peaks corresponding to –CH (5.3 ppm) and $-CH_3$ (1.5 ppm). The results of macromonomer synthesis are summarized in Table 1. The compositions of the co-polymers were determined by using the peak area ratios of peaks corresponding to –CH (5.3 ppm) and $-N-CH_3$ (3.1 ppm), as shown in Fig. 1. The molecular weights of PMLA were determined by gel-permeation chromatography (GPC; Jasco, Tokyo, Japan) in water/methanol (8:2, v/v). Shodex SB-804 (Showa Denko, Tokyo, Japan) was used as the separation column, and the weight-average molecular weight (M_w) and number-average molecular weight (M_n) were calculated using PEG standards as a reference.

2.5. Preparation of Polymer Hydrogel

Polymer solutions having various concentrations in the range 5.0–20 wt% were prepared (Table 3). Solutions (1 g) of PMLLA and PMDLA were mixed and allowed to stand for 24 h at room temperature (*ca.* 23°C). Gelation was confirmed by the loss of fluidity in the mixed solutions.

To quantitatively determine the gelation time, polymer solutions were placed into a stainless-steel cell (volume 2.0 ml) with two compartments separated by a vibration blade (1.7 cm^2) of the rheometer (Rheolograph Micro, Toyo-seiki, Tokyo, Japan). Immediately after the polymer solution was injected into the cell, the blade began to vibrate, mixing these polymer solutions to prepare the hydrogel (vibration amplitude 200 μm, frequency 20 Hz). The changes in the elastic modulus (G') and viscous modulus (G'') were recorded. The gelation time is defined as the time period at which the G' value corresponds to the G'' value.

2.6. Hydrolysis of Polymer Hydrogel

BSA containing 10 wt% FITC-labeled BSA (20 mg) was dissolved in phosphate buffered saline (PBS, pH 7.4) containing PMLLA. This solution was introduced into a glass tube; then, solutions of PBS in PMDLA were added to the solution, and the mixture was maintained at 5°C for 24 h to form the hydrogel. PBS solutions (9 ml) having various pH were added to the tube containing the hydrogel, and the system was maintained at 37°C. The fluorescence intensity of PBS containing the FITC-labeled BSA was measured with a fluorescence spectrophotometer (Jasco). The degradation ratio of the hydrogel was calculated as (fluorescence intensity of

Table 1.
Synthesis of oligo (lactic acid) macromonomers

Code	Chemical composition in feed (mmol)		[Lactide]/ [HEMA]	Chirality	Atmosphere	Pressure (atm)	Reprecipitation solvent	Polymerization degree (n)	Yield (%)
	HEMA	Lactide							
OLLA12	12	69	6.75	L	Argon	1.0	2-Propanol/ Hexane = 1:1	14	46
OLLA20	6.9	69	10	L	–	0.0013	Ethanol/ Hexane = 1:1	21	67
OLLA30	4.6	69	15	L	–	0.0013	Methanol	34	71
ODLA12	12	69	6.75	D	Argon	1.0	2-Propanol/ Hexane = 1:1	13	40
ODLA20	6.9	69	10	D	–	0.0013	Ethanol/ Hexane = 1:1	19	76
ODLA30	4.6	69	15	D	–	0.0013	Methanol	33	80

Polymerization degree was determined by ^{1}H-NMR.

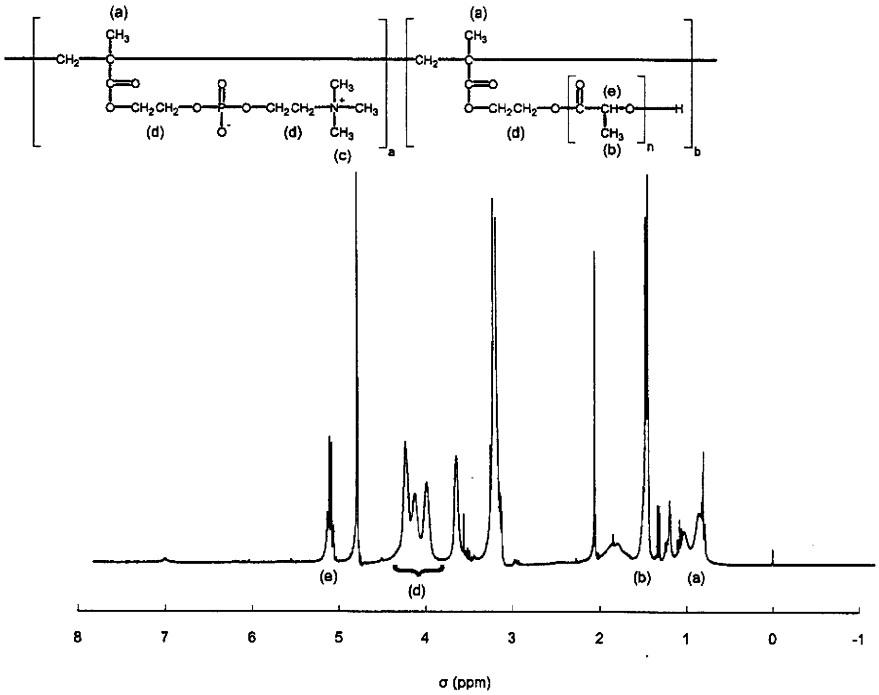

Figure 1. ^{1}H-NMR spectrum of a representative PMLA (X-PMDLA20-5).

PBS at a specific release time)/(theoretical maximum fluorescence intensity calculated from the amount of FITC-labeled BSA)× 100; this ratio was then plotted against time.

3. Results and Discussion

3.1. Synthesis of MPC Polymers with OLA as a Side-Chain

The MPC polymers (PMLA) were prepared to develop a water-soluble graft polymer with an oligo(lactic acid) side-chain. These polymers cause spontaneous gelation in aqueous solutions, which can be attributed to the formation of a stereocomplex between OLLA and ODLA. Biologically active substances can be incorporated in the polymer hydrogel during gelation, and the gel generally degrades under physiological conditions due to the non-enzymatic hydration of oligo(lactic acid) chains. During the degradation process, the biologically active substances incorporated in the hydrogel may be released. De Jong *et al.* reported self-assembled hydrogel using that system [4–6]. They grafted OLLA (dex-(L)lactate) and ODLA (dex-(D)lactate) to dextran and it is observed that the mixture of dex-(L)lactate aqueous solution and dex-(D)lactate aqueous solution formed a hydrogel. However, the various functions are required to the biomaterial and those are achieved by the controlled polymerization of the various monomers. From this point of view, polymethacrylate is

more suitable than polysaccharide because there are many methacrylate monomers and we can co-polymerize them. Moreover, it is well known that MPC polymers are biocompatible materials due to the relatively fewer protein-based interactions that occur at the tissue–implant interface [13–21, 28–30]. Thus, the use of MPC polymers offers interesting possibilities for obtaining injectable and biocompatible hydrogels [31–33].

Oligo(lactic acid) macromonomers were synthesized by a general method. Table 1 summarizes the polymerization results. The degree of polymerization of these macromonomers was approximately dependent on the feed ratio.

The polymerization of MPC and oligo(lactic acid) macromonomers proceeded homogeneously. The composition of each monomer unit in the MPC polymers corresponded to that in the feed monomer solution (Table 2). The polymers prepared using AIBN (A-PMLA) as the initiator did not dissolve but dispersed in water. On the other hand, the polymers formed by living radical polymerization using XDC (X-PMLA) as the iniferter were soluble in water (Scheme 2). The molecular weight distribution of A-PMLA was large. Small polymer particles dispersed in the aqueous medium may potentially cause inflammation and embolization. Therefore, A-PMLA was not suitable for application to medical materials. It is not entirely clear why the observed solubility of the polymers is different even if the MPC contents of the polymers are almost equal. However, one possible explanation may be the difference between the molecular weight distributions (M_n/M_w) of A-PMLA and X-PMLA. The M_n/M_w value of A-PMLA was larger than that of X-PMLA; thus, we could infer that A-PMLA included a water-insoluble portion due to its higher molecular weight. We considered that the molecular weight distribution of the polymer should be small in order to obtain stable hydrogels in an aqueous medium. Thus, we switched to the living radical polymerization method because using this method, we could regulate the M_n/M_w value. MPC polymers having 30 mol% MPC did not undergo biological reactions at the surface and thus showed excellent biocompatibility [15, 17, 29, 30]. The polymer used in this study contained approx. 90 mol% MPC, so we consider that this polymer has sufficient biocompatibility.

3.2. Effect of Polymer Concentration on Gelation Behavior

As shown in Fig. 2, spontaneous gelation occurred due to the mixing of aqueous solutions containing PMLLA and PMDLA, wherein the degree of polymerization of the oligo(lactic acid) macromonomer units was 12. The extent of gelation depended on the concentrations of both polymers, as summarized in Table 3. The lowest concentration required for gelation decreased with an increase in the molecular weight or the composition of oligo(lactic acid) macromonomer units. In previous studies, we investigated the formation of a stereocomplex between water-insoluble MPC polymers and enantiomeric poly(lactic acid) graft chains. Differential scanning calorimetry data and X-ray diffraction profiles of the precipitate from the polymer solution confirmed stereocomplex formation [11]. This suggests that the obtained

Table 2.
Synthesis of poly(MPC-graft-oligo(lactic acid))

Code	Macromonomer	Side-chain length	Monomer ratio in feed		Monomer unit composition in co-polymer[a]		Molecular weight ($\times 10^{-4}$)[b]	M_n/M_w[b]	Yield (%)	Water solubility[c]
			MPC	OL(D)LA	MPC	OL(D)LA				
A-PMLLA12-5	OLLA12	14	95	5	96	4	2.1	5.2	55	Turbid
A-PMLLA12-10	OLLA12	14	90	10	93	7	4.3	2.6	69	Turbid
A-PMLLA12-20	OLLA12	14	80	20	89	11	–	–	62	Turbid
A-PMLLA20-5	OLLA20	21	95	5	97	3	–	–	69	Turbid
A-PMLLA20-10	OLLA20	21	90	10	95	5	–	–	71	Turbid
A-PMLLA30-5	OLLA30	34	95	5	97	3	–	–	–	–
A-PMDLA12-5	ODLA12	13	95	5	95	5	–	–	59	Turbid
A-PMDLA12-10	ODLA12	13	90	10	93	7	–	–	66	Turbid
A-PMDLA12-20	ODLA12	13	80	20	88	12	–	–	48	Turbid
A-PMDLA20-5	ODLA20	19	95	5	97	3	2.7	2.4	85	Turbid
A-PMDLA20-10	ODLA20	19	90	10	94	6	–	–	83	Turbid
X-PMLLA20-5	OLLA12	20	95	5	97	3	1.6	2.0	64	Soluble
X-PMLLA20-10	OLLA12	20	90	10	93	7	2.4	1.7	–	Soluble
X-PMDLA20-5	ODLA12	20	95	5	96	4	2.7	2.4	–	Soluble
X-PMDLA20-10	ODLA12	20	90	10	92	8	2.1	1.4	–	Soluble

[a] Determined by ^{1}H-NMR.
[b] Determined with PEG standards.
[c] Concentration was 1 mg/ml.

Table 3.
Effect of polymer concentration on the gelation of A-PMLA and X-PMLA polymer systems

Code	L-polymer	D-polymer	Concentration of polymer (wt%)		
			5	10	20
SC12-5	A-PMLLA12-5	A-PMDLA12-5	Sol	Sol	Sol
SC12-10	A-PMLLA12-10	A-PMDLA12-10	Sol	Sol	Gel
SC12-20	A-PMLLA12-20	A-PMDLA12-20	Sol	Gel	Gel
SC20-5	A-PMLLA20-5	A-PMDLA20-5	Sol	Sol	Sol
SC20-10	A-PMLLA20-10	A-PMDLA20-10	Sol	Sol	Sol
X-SC20-5	X-PMLLA20-5	X-PMDLA20-5	Sol	Sol	Gel
X-SC20-10	X-PMLLA20-10	X-PMDLA20-10	Sol	Gel	Sol

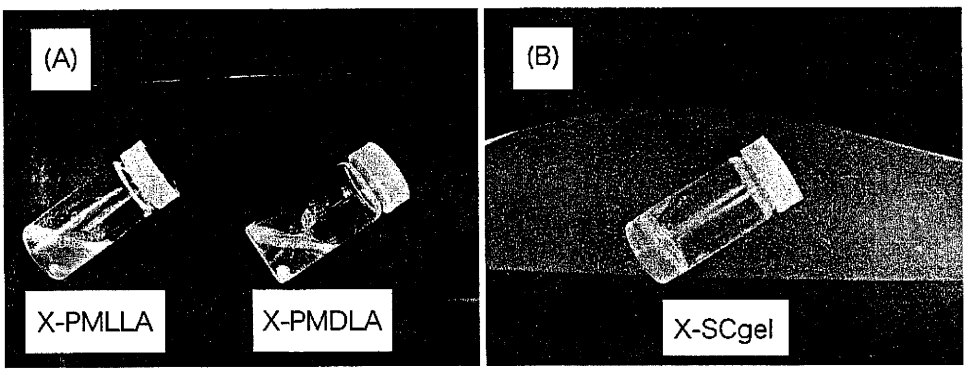

Figure 2. Pictures of gelation process resulting from the mixing of X-PMLLA and X-PMDLA (10 wt% aqueous solutions). (A) Aqueous solution of X-PMLLA20-10 (left) and X-PMDLA20-10 (right), (B) after mixing and standing for 24 h at room temperature.

hydrogel (X-SCgel) was produced by the formation of a stereocomplex between the L-form oligo(lactic acid) and the D-form oligo(lactic acid) as side-chains. On account of the hydrophobic nature of the oligo(lactic acid) side-chains, A-PMLA formed an aggregate in an aqueous medium. Therefore, it is necessary to organize the oligo(lactic acid) side-chains on the surface of the aggregate and for making easy interaction between these polymer chains. Oligo(lactic acid) macromonomers with 20 repeating lactic acid units had higher hydrophobicity than those with 12 repeating units, and the oligo(lactic acid) units were located inside the aggregate as cross-linking points. The gelation time of the X-SCgels depended on the polymer concentration. For instance, a mixture of 20 wt% polymers in the solution required 8.7 min for gelation, while a 15 wt% polymer solution required over 100 min (Fig. 3). Thus, we can control gelation time by changing polymer concentration.

3.3. Hydrolysis of the Hydrogel

The fluorescence intensity of the hydrogel containing PBS along with FITC-labeled BSA was measured to examine the degradation of the hydrogel. Since the perme-